Order, Criticality, and Excitations in the Extended Falicov-Kimball Model

S. Ejima,[1] T. Kaneko,[2] Y. Ohta,[2] and H. Fehske[1]
[1]Institut für Physik, Ernst-Moritz-Arndt-Universität Greifswald, 17489 Greifswald, Germany
[2]Department of Physics, Chiba University, Chiba 263-8522, Japan
(Received 1 August 2013; published 13 January 2014)

Using exact numerical techniques, we investigate the nature of excitonic (electron-hole) bound states and the development of exciton coherence in the one-dimensional half-filled extended Falicov-Kimball model. The ground-state phase diagram of the model exhibits, besides band-insulator and staggered orbital ordered phases, an excitonic insulator (EI) with power-law correlations. The criticality of the EI state shows up in the von Neumann entropy. The anomalous spectral function and condensation amplitude provide the binding energy and coherence length of the electron-hole pairs which, on their part, point towards a Coulomb interaction driven crossover from BCS-like electron-hole pairing fluctuations to tightly bound excitons. We show that while a mass imbalance between electrons and holes does not affect the location of the BCS-BEC crossover regime, it favors staggered orbital ordering to the disadvantage of the EI. Within the Bose-Einstein condensation (BEC) regime, the quasiparticle dispersion develops a flat valence-band top, in accord with the experimental finding for Ta_2NiSe_5.

DOI: 10.1103/PhysRevLett.112.026401 PACS numbers: 71.35.-y, 71.10.Hf

The formation and condensation of excitonic bound states of electrons and holes in semimetallic or semiconducting systems possessing a small band overlap or band gap is still—half a century after its theoretical prediction [1]—a topical issue in condensed matter physics [2–4]. If the binding energy of the excitons exceeds the overlap or gap, they may spontaneously condensate at low temperatures and drive the system into an excitonic insulator (EI) state. It has been pointed out that the semimetal-EI transition can be discussed in close analogy to the BCS superconductivity, whereas the semiconductor-EI transition is described in terms of a Bose-Einstein condensation (BEC) of preformed excitons [5]. Quite recently, as a candidate for the EI state, quasi-one-dimensional (1D) Ta_2NiSe_5 has raised and attracted much experimental attention [6]. Most notably, by angle-resolved photoemission spectroscopy, an extremely flat valence-band top at 40 K was observed and taken as a strong signature for the EI state to be formed out of "condensed" bound Ni $3d-$ Se $4p$ holes and Ta $5d$ electrons.

The detection of the EI state in Ta_2NiSe_5 has spurred multifaceted research activities with regard to the formation and possible condensation of excitons in 1D systems [7]. The minimal theoretical model in this respect is of the Falicov-Kimball type. While the original Falicov-Kimball model (FKM) describes localized f electrons interacting via a local Coulomb repulsion (U) with itinerant c electrons (t_c) if residing at the same Wannier site [8], an extended version takes into account also the direct nearest-neighbor f-electron hopping (t_f) [9]:

$$\mathcal{H} = -t_c \sum_{\langle i,j\rangle} c_i^\dagger c_j - t_f \sum_{\langle i,j\rangle} f_i^\dagger f_j + U \sum_i c_i^\dagger c_i f_i^\dagger f_i + \frac{D}{2} \sum_i (c_i^\dagger c_i - f_i^\dagger f_i). \quad (1)$$

Here, $\alpha_i^\dagger$ (α_i) denotes the creation (annihilation) operator of a spinless fermion in the $\alpha = \{c, f\}$ orbital at site i, and D is the level splitting between different α orbitals. In regard to the modeling of Ta_2NiSe_5, the half-filled-band case is of particular importance, and it has been shown theoretically that a direct f-c hopping (hybridization) is prohibited by symmetry reasons, at least between the valence-band top and conduction-band bottom [7].

For the original FKM, rigorous results were obtained only in infinite spatial dimensions by dynamical mean-field theory; see, e.g., reviews in Refs. [10,11]. The extended FKM (EFKM) [Eq. (1)] has been studied extensively in the context of EI formation for $D > 1$, using dynamical mean-field theory [12], random phase approximation [13], slave-boson [14], projective renormalization [15], and variational cluster [16] techniques, or purely numerical diagonalization procedures [17]. At the same time, the problem of electronic ferroelectricity, which is equivalent to the appearance of the EI in some theoretical models, has also attracted much attention [18,19]. This phenomenon was confirmed for the 2D EFKM by constrained path Monte Carlo simulations [20]. In 1D, however, true ferroelectric long-range order (the equivalent of a nonvanishing $\langle c^\dagger f\rangle$ expectation value in the limit of vanishing c-f-band hybridization) is not possible. This was demonstrated for the 1D FKM [21]. For the 1D EFKM, power-law critical (excitonic) correlations were observed instead [20]. Mean-field-based approaches [22] are unable to capture the EI state in 1D (despite their success for $D > 1$), mainly due to the lack of an order parameter associated with the breaking of the $U(1)$ symmetry. On this note, a thorough investigation of the ground-state and spectral properties of the 1D EFKM is still missing.

In this paper, we present a comprehensive numerical analysis of the 1D EFKM at half-filling. At first, we

determine the ground-state phase diagram from large-scale density-matrix renormalization group (DMRG) [23] calculations and identify—depending on the orbital level splitting—staggered orbital ordered (SOO) and band-insulator (BI) phases as well as an intervening critical EI state. Then, within the EI, we detect a crossover between BCS- and Bose-Einstein-type condensates monitoring the exciton-exciton correlation and exciton momentum distribution functions. Note that in our 1D setting, we use the term "condensate" to indicate a critical phase with power-law correlation decay. Finally, combining DMRG, Lanczos exact diagonalization (ED), and Green functions techniques [24], we study the anomalous spectral function and extract the correlation length and binding energy of the electron-hole pairs. This allows us to comment on the nature of the excitonic bound states preceding the condensation process and to discuss the effect of a mass imbalance between (c) electrons and (f) holes.

Examining the (large-U) strong-coupling regime gives a first hint of which phases might be realized in the 1D EFKM at zero temperature. To leading order, the EFKM can be mapped onto the exactly solvable spin-1/2 XXZ-Heisenberg model in a magnetic field $h = D$ aligned in the z direction [25]: $\mathcal{H}_{XXZ} = J\sum_j\{\Delta S^z_j S^z_{j+1} + (1/2)(S^+_j S^-_{j+1} + S^-_j S^+_{j+1})\} - h\sum_j S^z_j$, with $J = 4|t_f|t_c/U$ and $\Delta = (t_f^2 + t_c^2)/(2|t_f|t_c)$. The XXZ model exhibits three phases: the gapped antiferromagnetic (AF) phase, the critical gapless XY phase with central charge $c = 1$, and the ferromagnetic (FM) phase, where both transition lines, those between the AF and XY phases (h_{c_1}/J) and those between the XY and FM phases (h_{c_2}/J), follow from the Bethe ansatz [26]. Correspondingly, increasing the magnitude of the f-c level splitting D in the EFKM, we expect to find the following sequence of phases: (i) the SOO phase that matches the Ising-like AF phase in the XXZ model, (ii) an intermediate critical EI phase with finite excitonic binding energy, and (iii) a BI state, which is characterized by a filled (empty) f (c) band and related to the FM phase of the XXZ model. The phase boundary separating the EI and BI states is exactly known to be [27]

$$D_{c_2} = \sqrt{4(|t_f| + |t_c|)^2 + U^2} - U. \tag{2}$$

The complete phase diagram of the 1D EFKM is presented in Fig. 1. Symbols denote the DMRG BI-EI and EI-SOO transition points, which can be obtained from the energy differences

$$D_{c_2}(L) = E_0(L, 0) - E_0(L-1, 1) = -E_0(L-1, 1) \tag{3}$$

and

$$D_{c_1}(L) = E_0(L/2+1, L/2-1) - E_0(L/2, L/2), \tag{4}$$

respectively, in the course of a finite-size scaling analysis (see the inset). Here, $E_0(N_f, N_c)$ denotes the ground-state

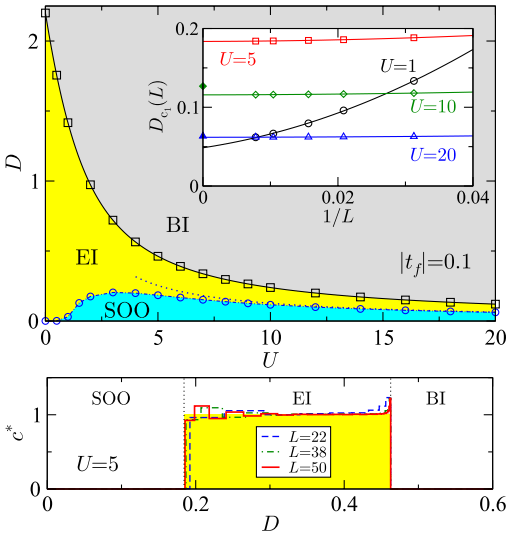

FIG. 1 (color online). Upper panel: Ground-state phase diagram of the half-filled 1D EFKM with $|t_f| = 0.1$. Here and in what follows, we take t_c as the unit of energy. Squares (circles) denote the EI-BI (EI-SOO) transition points D_{c_2} (D_{c_1}) obtained by the DMRG method with up to $L = 128$ sites and OBCs. The solid line gives the analytical solution (2) for the EI-BI boundary; the dotted line shows the strong-coupling result for the EI-SOO boundary. The finite-size scaling of $D_{c_1}(L)$ is illustrated by the inset (open symbols); here, the corresponding strong-coupling data are given by filled symbols. Lower panel: Central charge obtained at $U = 5$ for various L and PBCs. Criticality $c^* \sim 1$ is observed for the EI.

energy for a system with N_f f and N_c c electrons at $D = 0$. Note that Eq. (3) holds for both open and periodic boundary conditions (OBCs and PBCs), whereas Eq. (4) has to be evaluated with PBCs (if here OBCs were used, an extra factor 2 results: $D^{\mathrm{OBC}}_{c_1} = 2D_{c_1}$). For the DMRG runs performed in this work, we keep at least $m = 3200$ density-matrix eigenstates, which ensures a discarded weight smaller than 1×10^{-6}. The $D_{c_2}(L \to \infty)$ values demonstrate the accuracy of our DMRG calculations. Exact results for $D_{c_1}(L \to \infty)$ can only be obtained numerically, where a comparison with the dotted line reveals the limits of the strong-coupling approach [25]; see Fig. 1. The criticality of the EI phase—corresponding to the critical XY phase in the XXZ model with central charge $c = 1$—can be confirmed by the von Neumann entanglement entropy $S_L(\ell) = -\mathrm{Tr}_\ell(\rho_\ell \ln \rho_\ell)$ [with reduced density matrix $\rho_\ell = \mathrm{Tr}_{L-\ell}(\rho)$]. Numerically, the central charge is best estimated from the entropy difference [28,29]:

$$c^*(L) \equiv 3[S_L(L/2-1) - S_L(L/2)]/\ln\,[\cos(\pi/L)]. \tag{5}$$

Our results for c^*, displayed in the lower panel of Fig. 1 for $|t_f| = 0.1$ at $U = 5$, give clear evidence that $c^* \to 1$ in the EI, whereas we find $c^* = 0$ in the BI and SOO phases. Regrettably, $c^*(L)$ is strongly system size dependent near the EI-SOO transition.

Let us now discuss the nature of the EI state in more detail. For simplicity, we consider the case $t_f t_c < 0$, where two Fermi points ($\pm k_F$) exist for $U = 0$, provided D is sufficiently small (otherwise, a direct band gap emerges). As a signature of an excitonic Bose-Einstein condensate in 1D, one expects (i) a power-law decay of the correlations $\langle b_i^\dagger b_j \rangle$ with $b_i^\dagger = c_i^\dagger f_i$ and (ii) a divergence of the excitonic momentum distribution $N(q) = \langle b_q^\dagger b_q \rangle$ with $b_q^\dagger = (1/\sqrt{L}) \sum_k c_{k+q}^\dagger f_k$ for the state with the lowest possible energy (in the direct gap case at $q = 0$) due to the absence of true long-range order. Figure 2 supports these expectations: Whereas in the weak-coupling BCS regime ($U = 1$), $\langle b_i^\dagger b_j \rangle$ decays almost exponentially and $N(q)$ shows only a marginal system-size dependence (for all momenta), in the strong-coupling BEC regime close to the EI-BI transition ($U = 1.9$), $\langle b_i^\dagger b_j \rangle$ exhibits a rather slow algebraic decay of the excitonic correlations and $N(q = 0)$ becomes divergent as $L \to \infty$.

We note that the $\langle c^\dagger f \rangle$ expectation value is always zero for a 1D system in the absence of an explicit f-c-band hybridization. To examine the BCS-BEC crossover, we adopt a technique introduced for detecting the particle fluctuations of Cooper pairs in 2D systems [24]. That is, we consider the off-diagonal anomalous exciton Green function

$$G_{cf}(k,\omega) = \left\langle \psi_1 \left| c_k^\dagger \frac{1}{\omega + i\eta - \mathcal{H} + E_0} f_k \right| \psi_0 \right\rangle, \quad (6)$$

where $|\psi_0\rangle$ is the ground state $|N_f, N_c\rangle$ with fixed numbers of f and c electrons, $|\psi_1\rangle$ is the excited state $|N_f - 1, N_c + 1\rangle$, E_0 is the averaged energy of $|\psi_0\rangle$ and $|\psi_1\rangle$, and η is a broadening, and determine the corresponding spectral function $F(k,\omega) = (-1/\pi)\Im G_{cf}(k,\omega)$ that gives the condensation amplitude $F(k) = \langle \psi_1 | c_k^\dagger f_k | \psi_0 \rangle$. $F(k)$ can be directly computed by the ground-state DMRG method, taking into account an extra target state $|\psi_1\rangle$. From $F(k)$, the coherence length characterizing the excitonic condensate follows as

$$\xi^2 = \sum_k |\nabla_k F(k)|^2 / \sum_k |F(k)|^2. \quad (7)$$

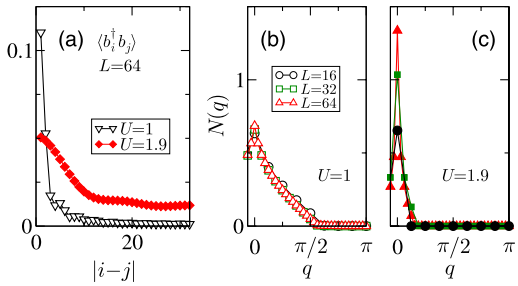

FIG. 2 (color online). (a) Exciton-exciton correlation function $\langle b_i^\dagger b_j \rangle$ and excitonic momentum distribution function $N(q)$ at (b) $U = 1$ and (c) $U = 1.9$ for $t_f = -0.1$, $D = 1$. Data are obtained by the DMRG for 1D L-site lattices with PBCs.

The binding energy of the excitons E_B can be also determined from diverse ground-state energies [17]:

$$E_B = E_0(N_f - 1, N_c + 1) + E_0(N_f, N_c) - E_0(N_f - 1, N_c) - E_0(N_f, N_c + 1). \quad (8)$$

Figures 3(a) and 3(b) show the anomalous spectral function $F(k,\omega)$ in the weak-coupling ($U = 1$) and strong-coupling ($U = 1.9$) regimes, respectively, where $D = 1$. In the former case, the EI arises from a semimetallic phase. As a consequence, most of the spectral weight of the quasiparticle excitations is located around the Fermi points $k = \pm k_F$, again indicating a BCS-type pairing of electrons and holes. Obviously, Fermi surface effects play no role for large U, where the Hartree shift drives the system in the semiconducting regime. Here, the excitation gap occurs at $k = 0$. Note that the gap between the lowest energy peaks in $F(k,\omega)$ is equal to the binding energy E_B given by Eq. (8). Figure 3(c) displays the frequency-integrated quantity $F(k)$. At $U = 1$, $F(k)$ exhibits a sharp peak at the Fermi momentum. Increasing U, the peak weakens and shifts to smaller momenta. Close to the EI-BI transition point $U = 1.9 \lesssim U_{c_2} = 1.92$, $F(k)$ has a maximum at $k = 0$ but is spread out in momentum space, indicating that the radius of electron-hole pairs becomes small in real space. Figure 3(d) gives the quasiparticle dispersion $E(k)$ derived from $A(k,\omega)$. Driving the BCS-BEC crossover by

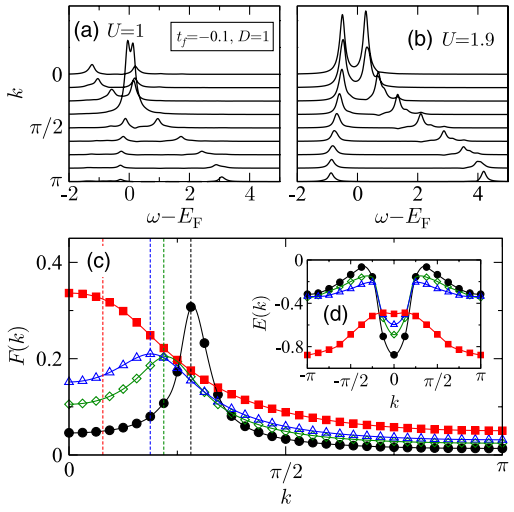

FIG. 3 (color online). Anomalous spectral function $F(k,\omega)$ in the 1D EFKM with (a) $U = 1$ and (b) $U = 1.9$, where $t_f = -0.1$, $D = 1$. Data are obtained by ED using $\eta = 0.1$, $L = 16$, and PBCs. Numerical results for (c) $F(k)$ and (d) $E(k)$ are shown for $U = 1$ (circles), 1.5 (diamonds), 1.7 (triangles), and 1.9 (squares). $F(k)$ is determined by the DMRG for $L = 64$ (PBC), whereas $E(k)$ is extracted from the lowest peaks of single-particle spectra $A(k,\omega)$ calculated by ED for $L = 16$ (PBC). Dashed lines in (c) mark the corresponding Fermi momenta $k_F = \pi N_c / L$ in the noninteracting limit.

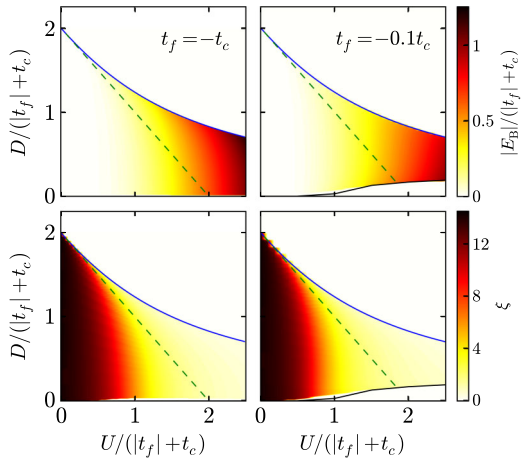

FIG. 4 (color online). Intensity plots of the binding energy $E_{\rm B}$ (upper panels; $L = 128$, OBC) and the coherence length ξ (lower panels; $L = 64$, PBC) in the rescaled $U/(|t_f| + t_c) - D/(|t_f| + t_c)$ plane. Data were calculated by the DMRG for $N_f > L/2$ (to avoid the AF state in the Hubbard model limit $|t_f| = 1$, $D = 0$). Solid lines denote the SOO-EI and EI-BI transition points in the thermodynamic limit (in the lower panels, the small uncolored slot just above the SOO-EI appears because $|E_B|$ and ξ are obtained here for a fixed finite system size). The dashed line $[U_{\rm BI}(D)]$ would separate the semimetallic and semiconducting phases if the EI is assumed to be absent.

increasing U, the peaks around $k = \pm k_F$ disappear as well as the notch around $k = 0$. Instead, a valence band with a flattop around $k = 0$ develops, just as observed, e.g., in quasi-1D Ta_2NiSe_5 [6].

Figure 4 shows the variation of the coherence length and the binding energy in the EI phase of the 1D EFKM with $|t_f| = 1$ (left panels) and 0.1 (right panels). At small U, the excitonic state is composed of electron-hole pairs having large spatial extension, leading to large values of ξ. E_B, on the other hand, is rather small, but increases exponentially with U. This typifies a BCS pairing mechanism. At large U, the binding increases linearly with U. Here, tightly bound spatially confined excitons acquire quantum coherence (with $\xi \ll 1$) in a Bose-Einstein condensation process.

We finally address the influence of a mass imbalance between f- and c-band quasiparticles. The EI phase is absent for $t_f = 0$. In the mass-symmetric case $|t_f| = t_c$, the 1D Hubbard model results for $D = 0$. Here, we cannot distinguish between the AF (with vanishing spin gap) and EI phases because both phases are critical. Therefore, in this limit, we have examined the 1D EFKM for $N_f > L/2$. To this end, both the U and D axes in Fig. 4 have been rescaled by $(|t_f| + t_c)$, as suggested by the EI-BI transition lines [Eq. (2)]. Indeed, we find that the EI phase shrinks as $|t_f|$ decreases. That is, the mass anisotropy gets stronger, which is simply a bandwidth effect, however, leading to a stronger Ising anisotropy. This, on their part, enlarges the SOO region, while the EI-BI phase boundary basically is unaffected. Importantly, the location of the BCS-BEC crossover, which can be derived from the intensity plots for E_B and ξ, does not change in this presentation. To expose correlation effects, we included in Fig. 4 the semimetallic-to-semiconducting transition line, assuming that the EI phase is absent. $U_{\rm BI}(D)$ can be obtained from the band gap Δ_c that depends linearly on U for fixed D: $\Delta_c(D) = U + 2(|t_f| + t_c) + U_{\rm BI}(D)$ [i.e., $U_{\rm BI}(D)$ scales again with $|t_f| + t_c$]. Apparently in the BCS-BEC crossover regime, a strong renormalization of the band structure due to the incipient f-c hybridization takes place.

To conclude, adopting the numerically exact density-matrix renormalization group technique, we examined the 1D EFKM and, most notably, proved the EI state shown to be critical. The complete ground-state phase diagram was derived and put into perspective, with the Bethe ansatz results obtained in the strong-coupling limit for the spin-1/2 XXZ chain. Besides the EI-to-band-insulator transition, the boundary between the EI and a phase with staggered orbital ordering was determined with high accuracy. The whole phase diagram of the 1D EFKM could be scaled by $|t_f| + t_c$; staggered orbital ordering appears only for small mass-imbalance ratios $|t_f|/t_c$. The absence of an order parameter prevents addressing the problem of excitonic condensation in 1D systems by the usual mean-field approaches. That is why we exploited the off-diagonal anomalous Green function. The related anomalous spectral function elucidates the different nature of the electron-hole pairing and condensation process at weak and strong couplings. At fixed level splitting, the binding energy between c electrons and f holes is exponentially small in the weak-coupling regime. It strongly increases as the Coulomb attraction increases. Concomitantly, the coherence length of the electron-hole pair condensate shortens. This unambiguously demonstrates a crossover from BCS-like electron-hole pairing to a Bose-Einstein condensation of preformed excitons. The quasiparticle band dispersion in the BEC regime exhibits a rather dispersionless valence band near $k = 0$, despite the fact that the expectation value $\langle c^\dagger f \rangle$ is zero because of the 1D setting. This result further supports the EI scenario for quasi-1D Ta_2NiSe_5, where the flat valence-band top was detected by angle-resolved photoemission spectroscopy experiments.

The authors would like to thank Y. Fuji, F. Göhmann, S. Nishimoto, K. Seki, T. Shirakawa, and B. Zenker for valuable discussions. S. E. and H. F. acknowledge funding by the DFG through SFB 652 Project B5. T. K. was supported by a JSPS Research Fellowship for Young Scientists. Y. O. acknowledges the Japanese Kakenhi Grant No. 22540363.

[1] N. F. Mott, Philos. Mag. **6**, 287 (1961); L. V. Keldysh and H. Y. V. Kopaev, Sov. Phys. Solid State **6**, 2219 (1965); D. Jérome, T. M. Rice, and W. Kohn, Phys. Rev. **158**, 462 (1967).

[2] J. Neuenschwander and P. Wachter, Phys. Rev. B **41**, 12693 (1990); P. Wachter, B. Bucher, and J. Malar, Phys. Rev. B **69**, 094502 (2004).
[3] H. Cercellier, C. Monney, F. Clerc, C. Battaglia, L. Despont, M. G. Garnier, H. Beck, P. Aebi, L. Patthey, H. Berger, and L. Forró, Phys. Rev. Lett. **99**, 146403 (2007); C. Monney, C. Battaglia, H. Cercellier, P. Aebi, and H. Beck, Phys. Rev. Lett. **106**, 106404 (2011).
[4] H. Min, R. Bistritzer, J. J. Su, and A. H. MacDonald, Phys. Rev. B **78**, 121401(R) (2008); T. Stroucken, J. H. Grönqvist, and S. W. Koch, J. Opt. Soc. Am. B **29**, A86 (2012).
[5] F. X. Bronold and H. Fehske, Phys. Rev. B **74**, 165107 (2006).
[6] Y. Wakisaka, T. Sudayama, K. Takubo, T. Mizokawa, M. Arita, H. Namatame, M. Taniguchi, N. Katayama, M. Nohara, and H. Takagi, Phys. Rev. Lett. **103**, 026402 (2009).
[7] T. Kaneko, T. Toriyama, T. Konishi, and Y. Ohta, Phys. Rev. B **87**, 035121 (2013); T. Kaneko, T. Toriyama, T. Konishi, and Y. Ohta, Phys. Rev. B **87**, 199902(E) (2013).
[8] L. M. Falicov and J. C. Kimball, Phys. Rev. Lett. **22**, 997 (1969); P. Farkašovský, Eur. Phys. J. B **20**, 209 (2001).
[9] C. D. Batista, Phys. Rev. Lett. **89**, 166403 (2002).
[10] T. Kennedy, Rev. Math. Phys. **06**, 901 (1994).
[11] J. K. Freericks and V. Zlatić, Rev. Mod. Phys. **75**, 1333 (2003).
[12] A. Taraphder, S. Koley, N. S. Vidhyadhiraja, and M. S. Laad, Phys. Rev. Lett. **106**, 236405 (2011).
[13] B. Zenker, D. Ihle, F. X. Bronold, and H. Fehske, Phys. Rev. B **85**, 121102(R) (2012).
[14] P. M. R. Brydon, Phys. Rev. B **77**, 045109 (2008); B. Zenker, D. Ihle, F. X. Bronold, and H. Fehske, Phys. Rev. B **81**, 115122 (2010).
[15] V. N. Phan, K. W. Becker, and H. Fehske, Phys. Rev. B **81**, 205117 (2010).
[16] K. Seki, R. Eder, and Y. Ohta, Phys. Rev. B **84**, 245106 (2011); T. Kaneko, K. Seki, and Y. Ohta, Phys. Rev. B **85**, 165135 (2012).
[17] T. Kaneko, S. Ejima, H. Fehske, and Y. Ohta, Phys. Rev. B **88**, 035312 (2013).
[18] T. Portengen, T. Östreich, and L. J. Sham, Phys. Rev. Lett. **76**, 3384 (1996).
[19] U. K. Yadav, T. Maitra1a, I. Singh, and A. Taraphder, Europhys. Lett. **93**, 47013 (2011).
[20] C. D. Batista, J. E. Gubernatis, J. Bonča, and H. Q. Lin, Phys. Rev. Lett. **92**, 187601 (2004).
[21] P. Farkašovský, Phys. Rev. B **59**, 9707 (1999); P. Farkašovský, Phys. Rev. B **65**, 081102 (2002).
[22] C. Schneider and G. Czycholl, Eur. Phys. J. B **64**, 43 (2008); P. Farkašovský, Phys. Rev. B **77**, 155130 (2008).
[23] S. R. White, Phys. Rev. Lett. **69**, 2863 (1992).
[24] Y. Ohta, T. Shimozato, R. Eder, and S. Maekawa, Phys. Rev. Lett. **73**, 324 (1994); Y. Ohta, A. Nakauchi, R. Eder, K. Tsutsui, and S. Maekawa, Phys. Rev. B **52**, 15617 (1995).
[25] G. Fáth, Z. Domański, and R. Lemański, Phys. Rev. B **52**, 13910 (1995).
[26] J. des Cloizeaux and M. Gaudin, J. Math. Phys. (N.Y.) **7**, 1384 (1966); M. Takahashi, *Thermodynamics of One-Dimensional Solvable Models* (Cambridge University Press, Cambridge, England, 1999).
[27] A. N. Kocharian and J. H. Sebold, Phys. Rev. B **53**, 12804 (1996).
[28] P. Calabrese and J. Cardy, J. Stat. Mech. (**2004**) P06002.
[29] S. Nishimoto, Phys. Rev. B **84**, 195108 (2011).